Journal of Sound and Vibration (1998) **217**(4), 665–689
Article No. sv981721

DYNAMIC INSTABILITY OF A GENERAL COLUMN UNDER A PERIODIC LOAD IN THE DIRECTION OF THE TANGENCY COEFFICIENT AT ANY AXIAL POSITION

M.-K. Yeh and C.-C. Chen

Department of Power Mechanical Engineering, *National Tsing Hua University*, *Hsinchu* 30043 *Taiwan*, *Republic of China*

(*Received* 4 *July* 1997, *and in final form* 7 *April* 1998)

The instability behavior of a parametrically excited column subjected to a periodic load at any axial position in the direction of the tangency coefficient was investigated analytically. For an inextensional neutral axis, the lateral and axial deflections of the column can be expressed as functions of natural mode shapes and the corresponding mode deflections of the column. The components of modal excitation force induced by the periodic load were found as well. The dynamic equation of the system was obtained by incorporating the modal excitation forces and the modal equations of the free transverse vibration of the column into the virtual work equation. The instability bandwidth of simple and combination resonances of a general column can be described systematically by the natural frequencies of the column, the amplitude of the excitation force and a set of instability bandwidth parameters. A general formula was obtained to determine directly the instability regions of the column system, while bypassing the procedures for reducing and solving the dynamic equation of the system.

Physical explanations are given for the behavior of simple and combination resonances. Examples for columns with various boundary conditions were described to indicate their instability regions and were found to agree quite well with the results by previous researchers.

1. INTRODUCTION

Parametrically excited instability of an elastic system is very important for dynamic problems. It has attracted a great amount of attention recently. Some researchers [1–3] used the perturbation method to solve various parametrically excited systems with multiple degrees of freedom. The problem of parametric instability of columns and beams can be roughly grouped, according to the method of excitation, into two categories.

The first category is the instability problem of columns or beams subjected to given periodic axial motion. Handoo and Sundararajan [4] studied analytically and experimentally the stability of cantilevered beams with varied bending stiffness, length, mass and carrying concentrated end mass under periodic axial motion at its fixed end. Saito and Koizumi [5] examined the parametric resonance of a

0022–460X/98/440665 + 25 $30.00/0

horizontal simply-supported beam with a concentrated mass at one end and subjected to periodic axial motion at the other end. Buffinton and Kane [6] studied the parametric instability of a beam periodically moving between two fixed simply supported points. Elmaraghy and Tabarrok [7] investigated the instability of a beam with encastré ends subjected to an axially periodic acceleration at one end.

The second category is the instability problem of columns or beams subjected to a given periodic axial load or tangential load. Evensen and Evan-Iwanowski [8] evaluated analytically and experimentally the principal resonance of a simply supported column under axially periodic loading at one end. Bolotin [9] observed experimentally the principal regions of instability of various columns under axial or tangential periodic loading at one end. Iwatsubo *et al*. [10] developed a numerical simulation procedure to find the principal regions of dynamic instability of a cantilevered column subjected to an axial and tangential periodic end loading. Subsequently, Iwatsubo and coworkers [11, 12] investigated numerically the simple and combination resonances of a periodically time-varying continuous system; they applied the method to solve the problems of cantilevered, simply supported, clamped–clamped, and clamped–simply supported columns under axial or tangential periodic loads at one end of the column. Nayfeh and Mook [2] used the perturbation method to solve the problem of a cantilevered column subjected to a periodically excited tangential force at the free end of the column. Sato *et al*. [13] examined the instability behavior of a simply supported horizontal beam carrying a concentrated mass under axial periodic load at one end; they discussed the effect caused by the weight and position of the concentrated mass on the instability of beams. Chen and Yeh [14] investigated a cantilevered column subjected to periodic loads in varying direction of the tangency coefficient at the free end of the column.

Although many studies have concentrated on the problem of the second category, little information is available on the load applied on the more general column. In this work, a general formula used to describe the regions of the simple and combination resonances of a column under periodic load in varying directions of the tangency coefficient at any axial position has been developed. The column may have non-uniform cross-sections, non-homogeneous materials, or various supported conditions. The advantage of this method is that the instability regions of a general column can be easily determined from its natural frequencies and mode shapes.

2. THE PROBLEM

As shown in Figure 1, a column is subjected to a periodic external force, $f(t) = f_0 \cos \omega t$, at an arbitrary point P on the neutral axis of the column in the direction of tangency coefficient. The neutral axis of the column is originally straight. The cross-section and material properties of the column are symmetric about the x-z plane and may vary along the length of the column. The column has length L, mass M, mass per unit length $\rho(x)$, and bending rigidity $E(x)I(x)$. At an arbitrary time t, the point P moves to point P′. The deflections in the x and y directions are $u(x, t)$ and $v(x, t)$, respectively. The direction of the external force,

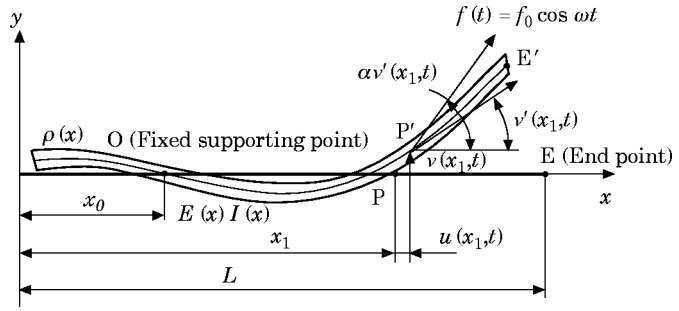

Figure 1. Parametric excitation of a general column.

i.e., the direction of the tangency coefficient, was obtained by multiplying the slope of point P′, $v'(x_1, t)$, by a tangency coefficient α as $\alpha v'(x_1, t)$. The fixed supporting point of the column is point O. The x co-ordinates of point O and point P are x_0 and x_1 respectively. In this study, the following assumptions are made: (1) The neutral axis of the column is inextensible; (2) Only small deflections in the x and y directions are considered; (3) The gravitational effects are neglected; (4) The damping effects are neglected.

3. PARAMETRIC EXCITATION OF A GENERAL COLUMN

For the general column, as shown in Figure 1, the free vibration equation of the column in the transverse direction is

$$\partial^2/\partial x^2(E(x)I(x)\,\partial^2 v/\partial x^2) + \rho(x)\,\partial^2 v/\partial t^2 = 0. \tag{1}$$

Let the natural frequencies of the column be ω_n and the corresponding mode shape functions $\phi_n(x)$. The transverse deflection $v(x, t)$ can be expressed in terms of the mode shapes $\phi_n(x)$ and the corresponding modal deflection components $V_n(t)$ as

$$v(x, t) = \sum_{n}^{\infty} \phi_n(x) V_n(t). \tag{2}$$

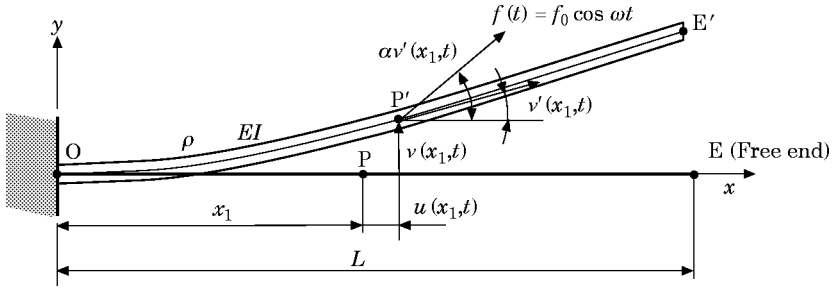

Figure 2. Parametric excitation of a cantilevered column. $\lambda_1 = 1{\cdot}8751040$; $\lambda_2 = 4{\cdot}6940910$; $\lambda_3 = 7{\cdot}8547575$; $\lambda_4 = 10{\cdot}995541$; $\bar{\omega}_n = \lambda_n^2/\lambda_1^2$; $\phi_n(\eta) = \sqrt{1/\rho L}\ \{\cosh(\lambda_n\eta) - \cos(\lambda_n\eta) - k_n [\sinh(\lambda_n\eta) - \sin(\lambda_n)]\}$, where $k_n = [\cosh(\lambda_n) + \cos(\lambda_n)]/[\sinh(\lambda_n) + \sin(\lambda_n)]$.

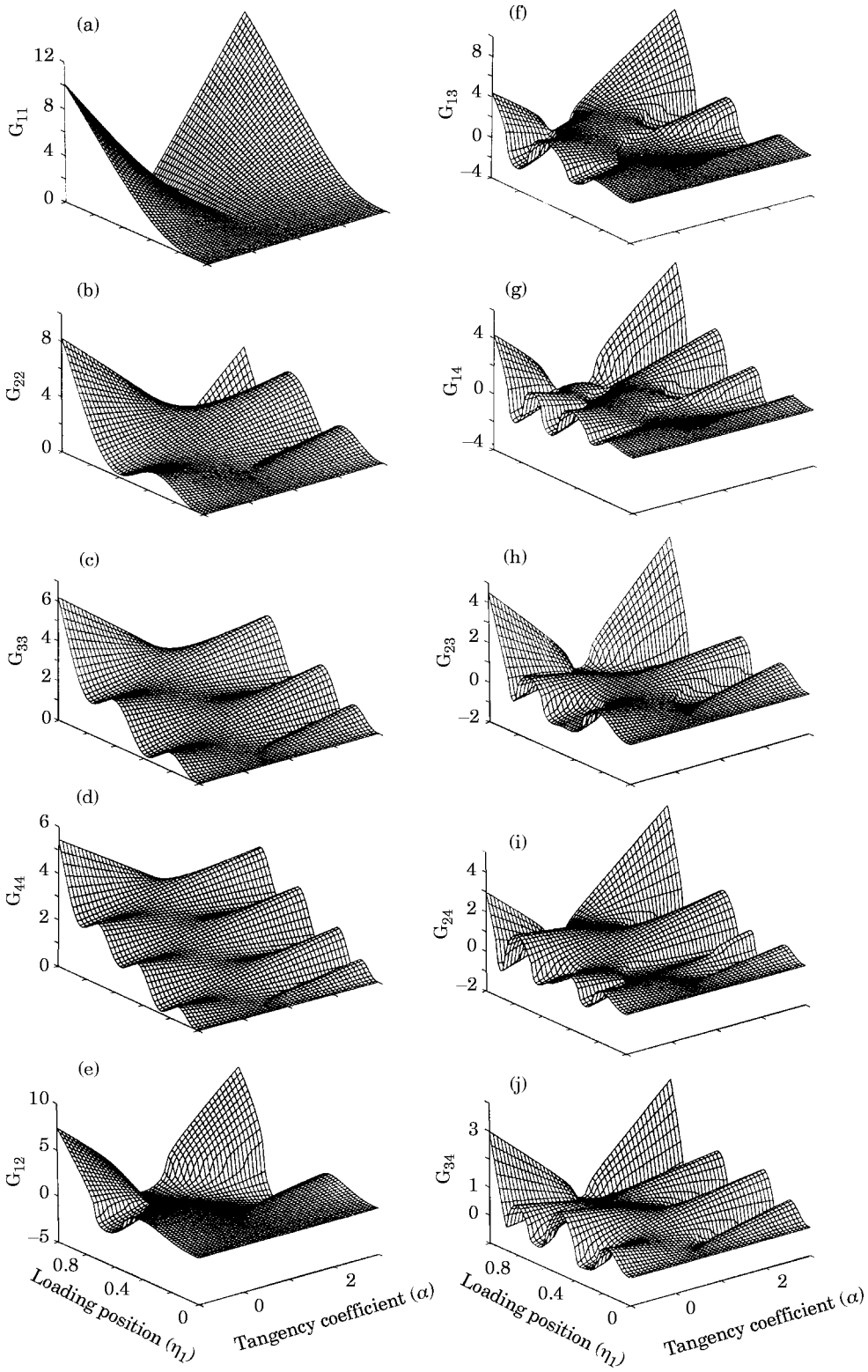

Figure 3. Instability bandwidth parameter, G_{nn}, of a cantilevered column.

For convenience, the mode shape functions $\phi_n(x)$ are chosen to be a set of orthonormal functions as $\int_0^L \rho(x)\phi_n(x)\phi_m(x)\,\mathrm{d}x = \delta_{nm}$. The governing equation of the free transverse vibration of the column can be expressed by modal deflection components $V_n(t)$ as

$$\ddot{V}_n(t) + \omega_n^2 V_n(t) = 0. \tag{3}$$

Bt assuming an inextensional neutral axis and small deflections in the x and y directions, the horizontal displacement of the loading point P, $u(x_1, t)$, can be expressed approximately by the transverse displacement $v(x, t)$ as

$$u(x_1, t) = -\tfrac{1}{2}\int_{x_0}^{x_1} v'^2(x, t)\,\mathrm{d}x, \tag{4}$$

where x_0 and x_1 are the x co-ordinates of fixed supporting point O and loading point P, respectively. The modal excitation force Q_n induced by the external load $f(t)$ can be obtained from virtual work as in Chen and Yeh [14]

$$Q_n = -f_0 \cos \omega t \sum_m \left[\int_{x_0}^{x_1} \phi_n'(x)\phi_m'(x)\,\mathrm{d}x - \alpha\phi_n(x_1)\phi_m'(x_1)\right] V_m(t). \tag{5}$$

The governing equation of the forced vibration of the column system, as shown in Figure 1, can be expressed as

$$\ddot{V}_n(t) + \omega_n^2 V_n(t) = Q_n, \qquad n = 1, 2, 3, \ldots, \tag{6}$$

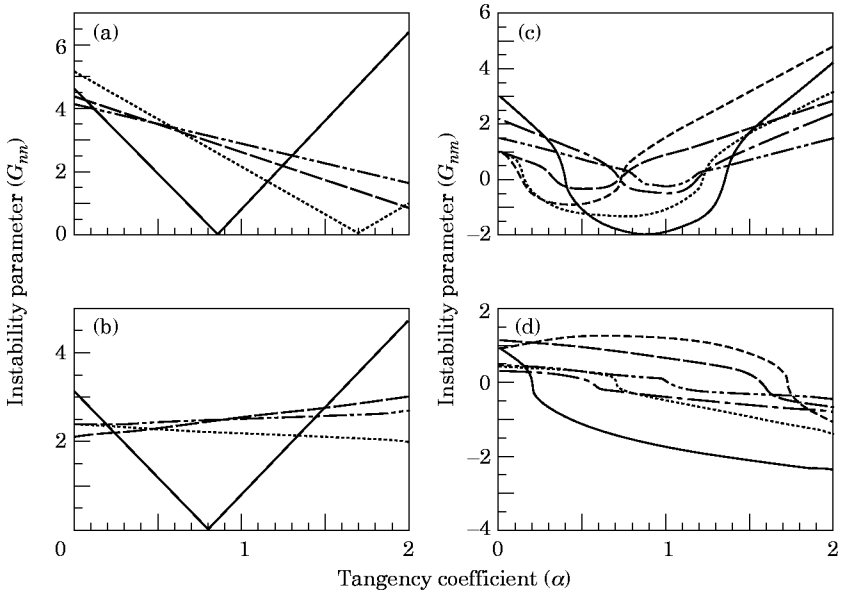

Figure 4. Instability bandwidth parameter, G_{nm}, of a cantilevered column versus tangency coefficient; α: (a) $\eta_1 = 1{\cdot}0$; ——, G_{11}; ----, G_{22}; —·—·—, G_{33}; —· · ·—, G_{44}: (b) As for Figure 4(a) except $\eta_1 = 0{\cdot}8$: (c) $\eta_1 = 1{\cdot}0$; ——, G_{12}; ----, G_{13}; · · · · , G_{14}; —·—, G_{23}; —·— , G_{24}; —· · ·—, G_{34}: (d) As for Figure 4(c) except for $\eta_1 = 0{\cdot}8$.

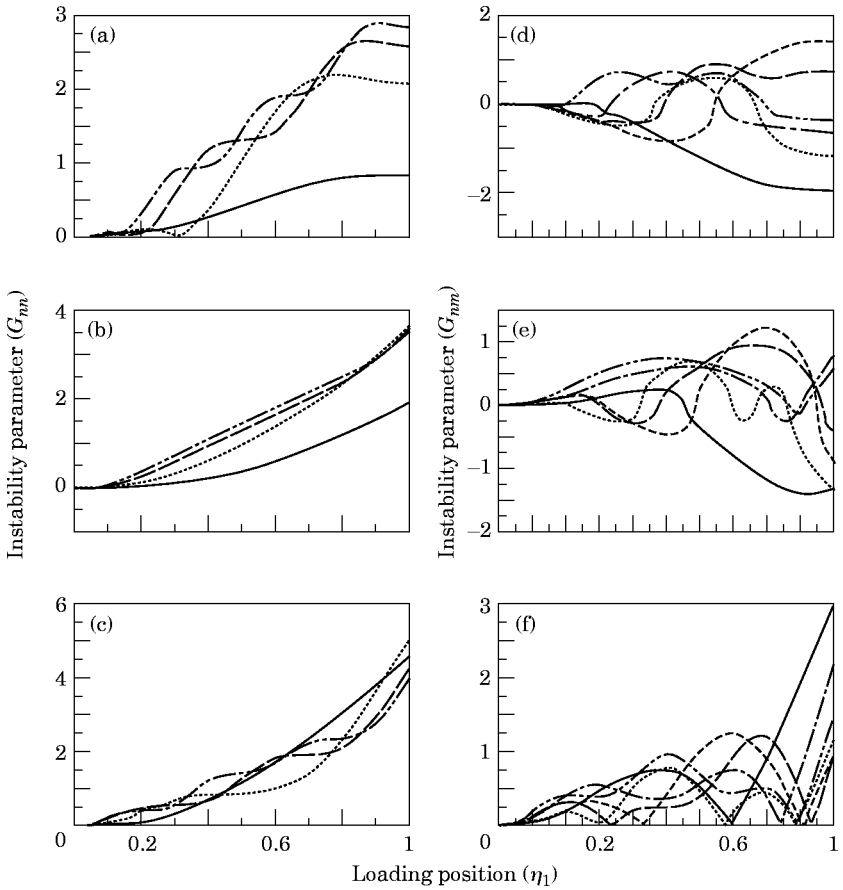

Figure 5. Instability bandwidth parameter, G_{nm}, of a cantilevered column versus loading position, η_1: (a, d), $\alpha = 1{\cdot}0$; (b, e) $\alpha = 0{\cdot}5$; (c, f) $\alpha = 0{\cdot}0$. Key: (a, b, c) as for Figure 4(a); (d, e, f) as for Figure 4(c).

or

$$\ddot{V}_n(t) + \omega_n^2 V_n(t) + f_0 \cos \omega t \sum_m \left[\int_{x_0}^{x_1} \phi_n'(x)\phi_m'(x)\,\mathrm{d}x - \alpha\phi_n(x_1)\phi_m'(x_1) \right] V_m(t) = 0. \tag{7}$$

The non-dimensionalized variables used are: $\tau = \omega_1 t$, time; $\eta = x/L$, general co-ordinate; $\eta_0 = x_0/L$, the co-ordinate of fixed supporting point O; $\eta_1 = x_1/L$, the co-ordinate of loading point P; $\bar{\omega}_n = \omega_n/\omega_1 \quad n = 1, 2, 3, \ldots$, the natural frequencies; $\bar{\omega} = \omega/\omega_1$, the excitation frequency; $\epsilon = f_0/2ML\omega_1^2$, the amplitude of the excitation force.

Equation (7) can be rewritten in non-dimensionalized form as

$$\ddot{V}_n(\tau) + \bar{\omega}_n^2 V_n(\tau) + 2\epsilon \cos(\bar{\omega}\tau) \sum_m^{\infty} f_{nm} V_m(\tau) = 0, \qquad n = 1, 2, 3, \ldots, \tag{8}$$

where

$$f_{nm} = M\left[\int_{\eta_0}^{\eta_1} \phi_n'(\eta)\phi_m'(\eta)\,\mathrm{d}\eta - \alpha\phi_n(\eta_1)\phi_m'(\eta_1)\right], \qquad n, m = 1, 2, 3, \ldots, \tag{9}$$

are the parametric excitation coefficients which are functions of the normalized natural mode shape $\phi_n(\eta)$, derivatives of mode shape $\phi_n'(\eta)$, $\phi_m'(\eta)$, mass of the column M, the tangency coefficient α, the co-ordinates of the fixed supporting point, η_0, and the loading point, η_1.

Equation (8) is a standard Mathieu's equation with multiple degrees of freedom used to express the dynamic behavior of a column subjected to a periodic load at an arbitrary point on the axis of column in the direction of the tangency coefficient. Once the coefficients f_{nm} are obtained, the instability bandwidth of simple and combination resonances of equation (8) can be determined by using

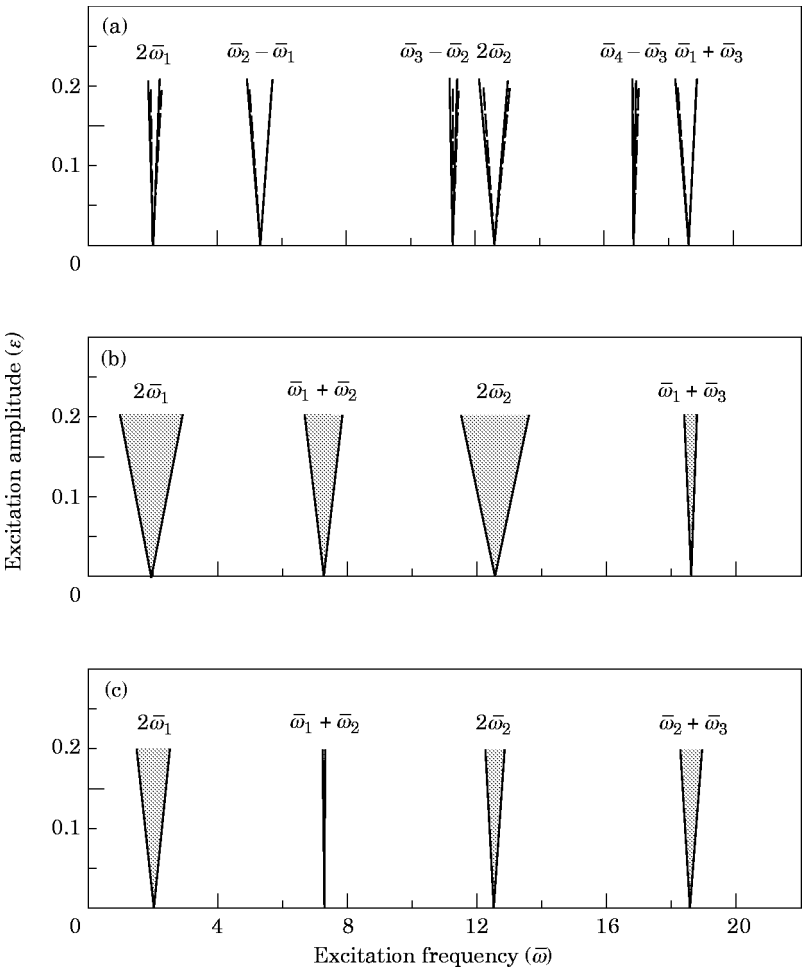

Figure 6. Parametric instability regions of a cantilevered column for various tangency coefficients, α, and loading position, η_1: (a) $\eta_1 = 1{\cdot}0$, $\alpha = 1{\cdot}0$; (b) $\eta_1 = 1{\cdot}0$, $\alpha = 0{\cdot}0$; (c) $\eta_1 = 0{\cdot}7$, $\alpha = 0{\cdot}0$: Key: ——, present; ----, Nayfeh and Mook [2]; - - -, Iwatsubo *et al*. [12].

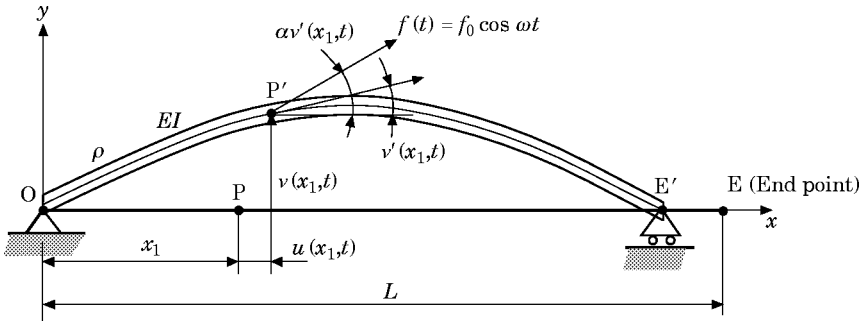

Figure 7. Parametric excitation of a simply supported column. $\lambda_n = n\pi$; $\bar{\omega}_n = \lambda_n^2/\lambda_1^2$; $\phi_n(\eta) = \sqrt{2/\rho L}\,\sin(\lambda_n \eta)$.

the amplitude of the excitation force ϵ, the natural frequencies of the column $\bar{\omega}_n$, $\bar{\omega}_m$, and the instability bandwidth parameter [14]

$$G_{nm} = \text{sign}\,(f_{nm} f_{mn})[|f_{nm} f_{mn}|/\bar{\omega}_n \bar{\omega}_m]^{1/2}, \tag{10}$$

as:

(1) When $n = m$, a simple resonance occurs in the region centered at $\bar{\omega} = 2\bar{\omega}_n$ with bandwidth $2\epsilon G_{nn}$.

(2) When $n \neq m$ and $G_{nm} > 0$, a combination resonance of the sum type occurs in the region centered at $\bar{\omega} = \bar{\omega}_n + \bar{\omega}_m$ with bandwidth $2\epsilon G_{nm}$.

(3) When $n \neq m$, $\bar{\omega}_n > \bar{\omega}_m$, and $G_{nm} < 0$, a combination resonance of difference type occurs in the region centered at $\bar{\omega} = \bar{\omega}_n - \bar{\omega}_m$ with bandwidth $2\epsilon G_{nm}$.

For a general system, as shown in Figure 1, the natural frequencies of the column $\bar{\omega}_n$ and the corresponding mode shape functions $\phi_n(\eta)$ can be found by using an analytical method, numerical method, or experimental method. Once the natural frequencies and mode shapes are given, the parametric excitation coefficient f_{nm} in equation (9) and the instability bandwidth parameter G_{nm} in equation (10) can be calculated to determine the instability regions. The procedures of deriving and solving the dynamic equation of the system can be bypassed when evaluating all the regions of simple and combination resonances.

In addition, from equations (9) and (10), the system has the following characteristics:

(1) When the tangency coefficient $\alpha = 0$, i. e., the direction of the periodic load is parallel to the undeformed horizontal axis, all of the parametric excitation coefficients f_{nm} are symmetric; therefore, all of the instability bandwidth parameters G_{nm} are greater than or equal to zero. Physically, all of the combination resonances, if occurring, will be of the sum type.

(2) When $\alpha = 0$ the parametric excitation coefficients f_{nn} in equation (9) become

$$f_{nn} = M \int_{\eta_0}^{\eta_1} \phi_n'^2(\eta)\,\mathrm{d}\eta, \qquad n = 1, 2, 3, \ldots, \tag{11}$$

in which η_0 and η_1 are the co-ordinates of the fixed supporting point O and the loading point P respectively, and the integrand $\phi_n'^2(\eta)$ is greater than or equal to

zero. Thus, the values of f_{nn} and G_{nn} increase as the distance between point P and point O increases. Physically, the instability bandwidth of simple resonance $2\epsilon G_{nn}$ increases with increase of the distance between point P and point O as the amplitude of excitation ϵ is kept constant.

(3) When the loading point P is located at a supporting point so that its transverse deflection $v(\eta_1, \tau)$ or slope $v'(\eta_1, \tau)$ vanishes, from equation (9), one has

$$f_{nm} = M \int_{\eta_0}^{\eta_1} \phi_n'(\eta)\phi_m'(\eta)\, \mathrm{d}\eta, \qquad n, m = 1, 2, 3, \ldots . \tag{12}$$

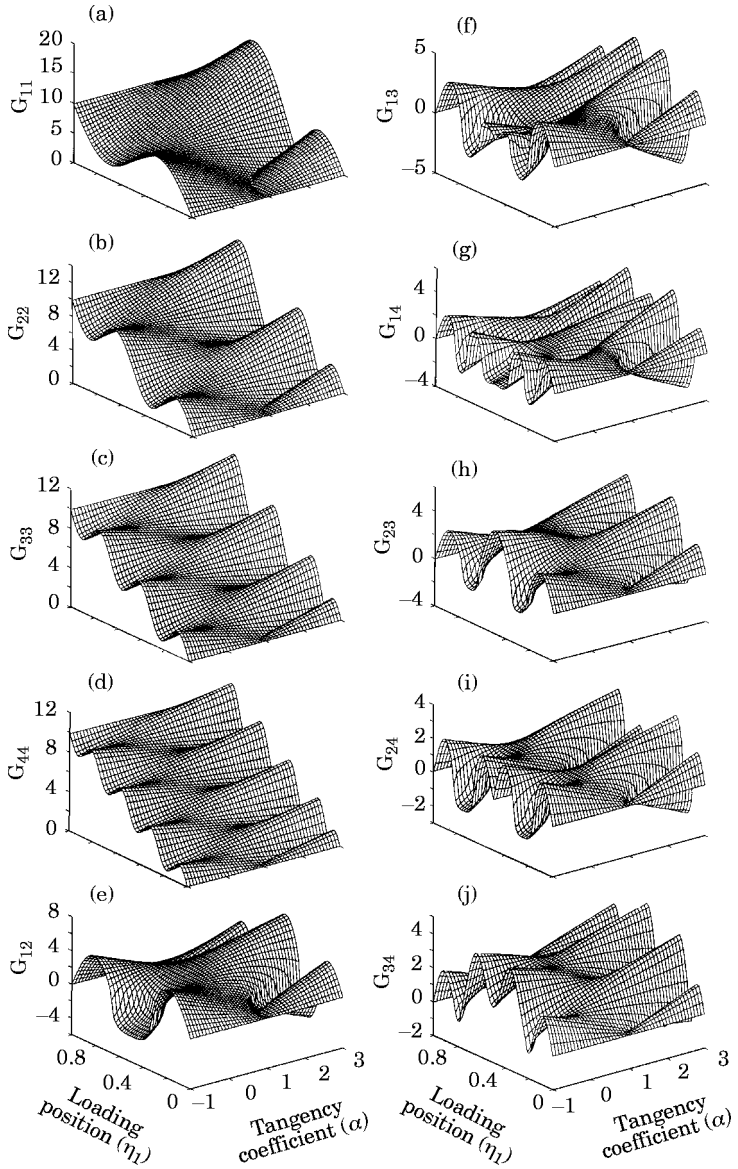

Figure 8. Instability bandwidth parameter, G_{nm}, of a simply supported column.

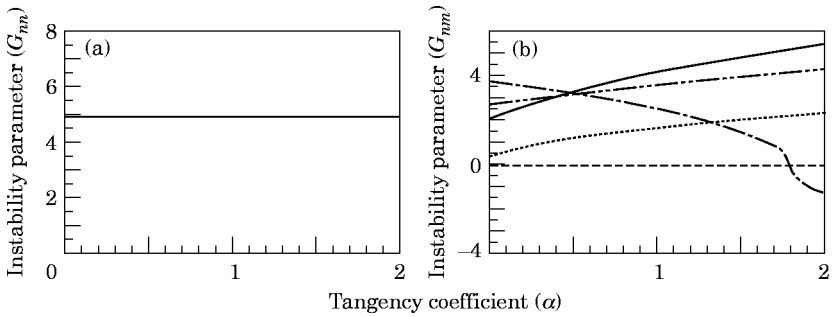

Figure 9. Instability bandwidth parameter, G_{nm}, of a simply supported column versus tangency coefficient, α, ($\eta_1 = 0{\cdot}5$). Key: (a) as for Figure 4(a); (b) as for Figure 4(c).

Therefore, all of the parametric excitation coefficients f_{nm} are symmetric and are not functions of the tangency coefficient α; all of the instability bandwidth parameters G_{nm} are greater than or equal to zero. Physically, all of the combination resonances, if occurring, will be of the sum type and the instability bandwidth $2\epsilon G_{nm}$ are independent of the tangency coefficient α.

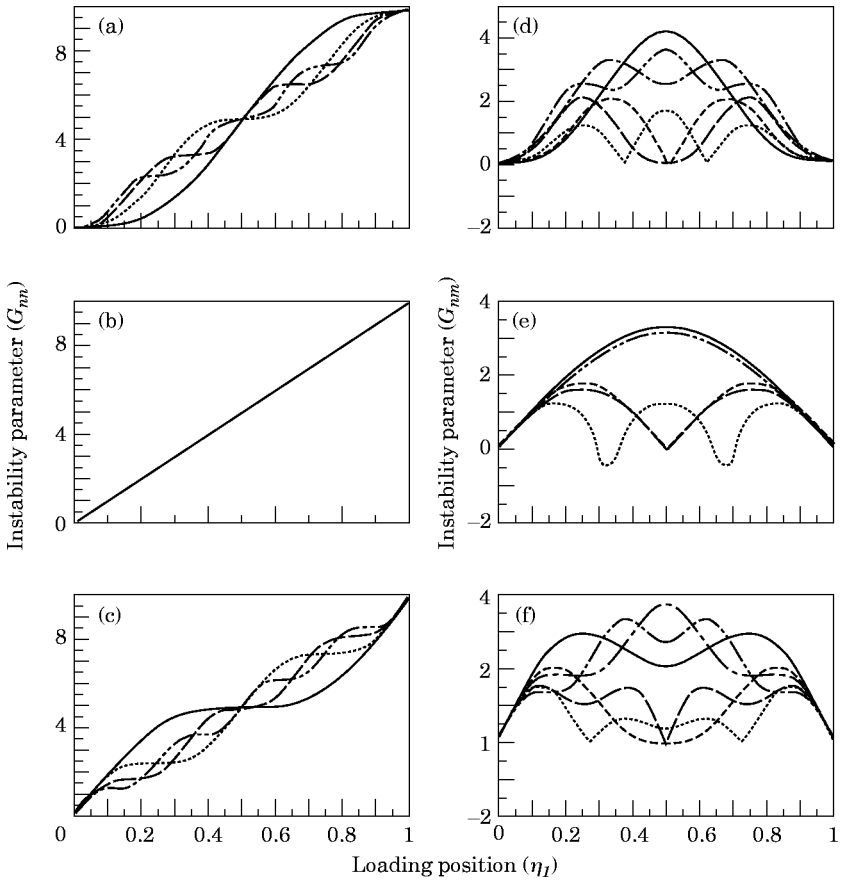

Figure 10. Instability bandwidth parameter, G_{nm}, of a simply supported column versus loading position, η_1. α values and key identical to Figure 5.

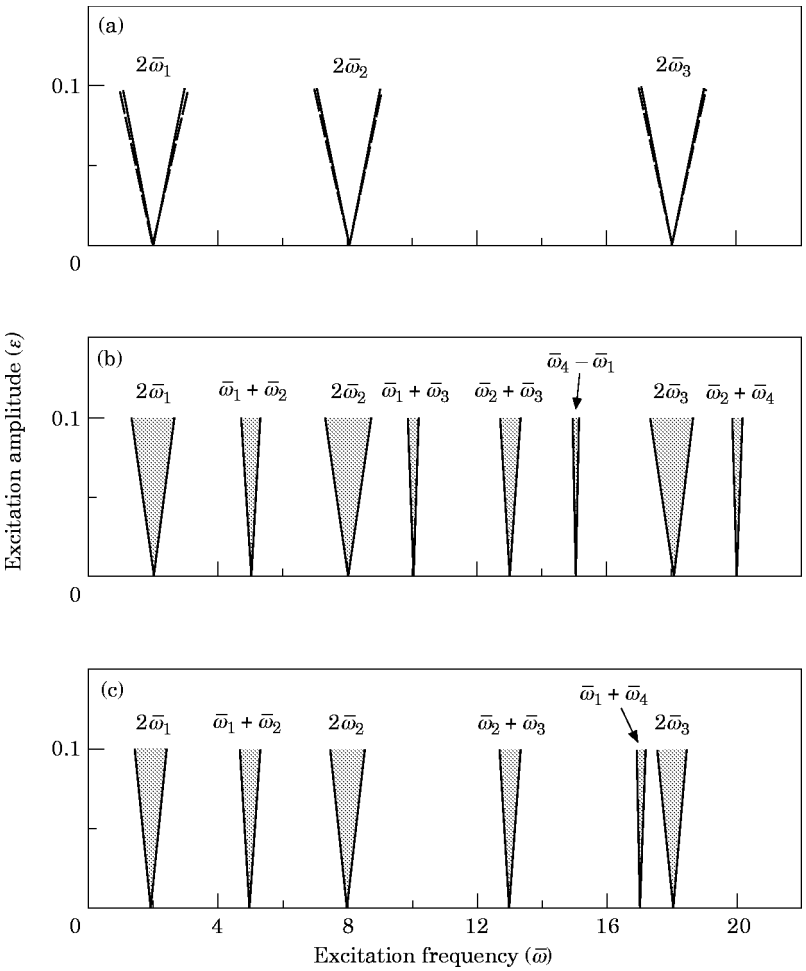

Figure 11. Parametric instability regions of a simply supported column for various tangency coefficient, α, and loading position, η_1: (a) $\eta_1 = 1{\cdot}0$, α arbitrary; (b) $\eta_1 = 0{\cdot}67$, $\alpha = 0{\cdot}5$; (c) $\eta_1 = 0{\cdot}5$, $\alpha = 0{\cdot}5$. Key: ——, present; ----, Iwatsubo *et al*. [12].

(4) When the loading point P is located at the node point of the nth mode shape, $(\phi_n(\eta_1) = 0)$, or at the zero-slope point of the nth mode shape, $(\phi_n'(\eta_1) = 0)$, from equation (9), f_{nn} is independent of the tangency coefficient α; thus the instability parameter G_{nn} of simple resonance is not a function of the tangency coefficient α.

(5) When the node points of the nth and the mth mode shapes or the zero-slope points of the nth and the mth mode shapes overlap and the loading point is located at that point, from equation (9), f_{nm} is independent of the tangency coefficient α; thus the instability parameter G_{nm} of combination resonance is independent of the tangency coefficient α and G_{nm} is greater than or equal to zero.

4. PHYSICAL EXPLANATIONS OF PARAMETRIC INSTABILITY

The instability behavior obtained above is explained physically as follows:

4.1. SIMPLE RESONANCE

Consider the oscillation of the nth mode of equation (8) as

$$\ddot{V}_n(\tau) + \bar{\omega}_n^2 V_n(\tau) = -2\epsilon \cos(\bar{\omega}\tau) f_{nn} V_n(\tau) + RT, \tag{13}$$

in which RT represents the regular terms that produce no resonant conditions. Multiplying equation (13) by $\dot{V}_n$ and neglecting the regular terms (RT), one obtains the energy form of equation (13)

$$\mathrm{d}/\mathrm{d}t(\tfrac{1}{2}\dot{V}_n^2 + \tfrac{1}{2}\bar{\omega}_n^2 V_n^2) = -2\epsilon \cos(\bar{\omega}\tau) f_{nn} V_n \dot{V}_n. \tag{14}$$

The term on the left side, $\mathrm{d}/\mathrm{d}t(\frac{1}{2}\dot{V}_n^2 + \frac{1}{2}\bar{\omega}_n^2 V_n^2)$, represents the time rate change of the total energy of the nth mode and the term on the right side, $-2\epsilon \cos(\bar{\omega}\tau) f_{nn} V_n \dot{V}_n$, represents the power done on the nth mode by the generalized force $-2\epsilon \cos(\bar{\omega}\tau) f_{nn} V_n$. As ϵ approaches zero, the power done by the generalized force is small, and thus in a short time interval the oscillation of $V_n(\tau)$ can be expressed approximately as

$$V_n(\tau) \cong \overline{V}_n \cos(\bar{\omega}_n \tau + \theta_n), \tag{15}$$

where $\overline{V}_n$, θ_n are the amplitude and phase of $V_n(\tau)$ respectively. When the excitation frequency $\bar{\omega}$ approaches twice the natural frequency $2\bar{\omega}_n$, the power input of the generalized force becomes

$$\begin{aligned} -2\epsilon f_{nn} V_n \dot{V}_n \cos(\bar{\omega}\tau) &\cong \epsilon f_{nn} \overline{V}_n^2 \bar{\omega}_n \cos(2\bar{\omega}_n \tau) \sin(2\bar{\omega}_n \tau + 2\theta_n) \\ &= \tfrac{1}{2}\epsilon f_{nn} \overline{V}_n^2 \bar{\omega}_n [\sin(4\bar{\omega}_n \tau + 2\theta_n) + \sin(2\theta_n)]. \end{aligned} \tag{16}$$

The average power of the first term on the right side of equation (16), $\frac{1}{2}\epsilon f_{nn} \overline{V}_n^2 \bar{\omega}_n \sin(4\bar{\omega}_n \tau + 2\theta_n)$, is equal to zero, and the average power of the second term on the right side, $\frac{1}{2}\epsilon f_{nn} \overline{V}_n^2 \bar{\omega}_n \sin(2\theta_n)$, is constant. When the second term is positive, the power input to the nth mode is positive and the total energy of the nth mode increases continuously. Therefore, the system becomes unstable when the excitation frequency $\bar{\omega}$ is near $2\bar{\omega}_n$.

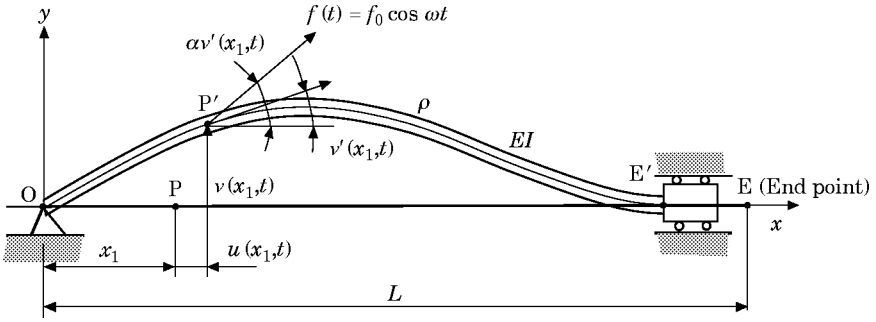

Figure 12. Parametric excitation of a clamped–simply supported column. $\lambda_1 = 3{\cdot}92660$; $\lambda_2 = 7{\cdot}06859$; $\lambda_3 = 10{\cdot}21018$; $\lambda_4 = 13{\cdot}135177$; $\bar{\omega}_n = \lambda_n^2/\lambda_1^2$; $\phi_n(\eta) = \sqrt{2/\rho L}[\sin(\lambda_n \eta) - k_n \sinh(\lambda_n \eta)]$ where $k_n = \sin(\lambda_n)/\sinh(\lambda_n)$.

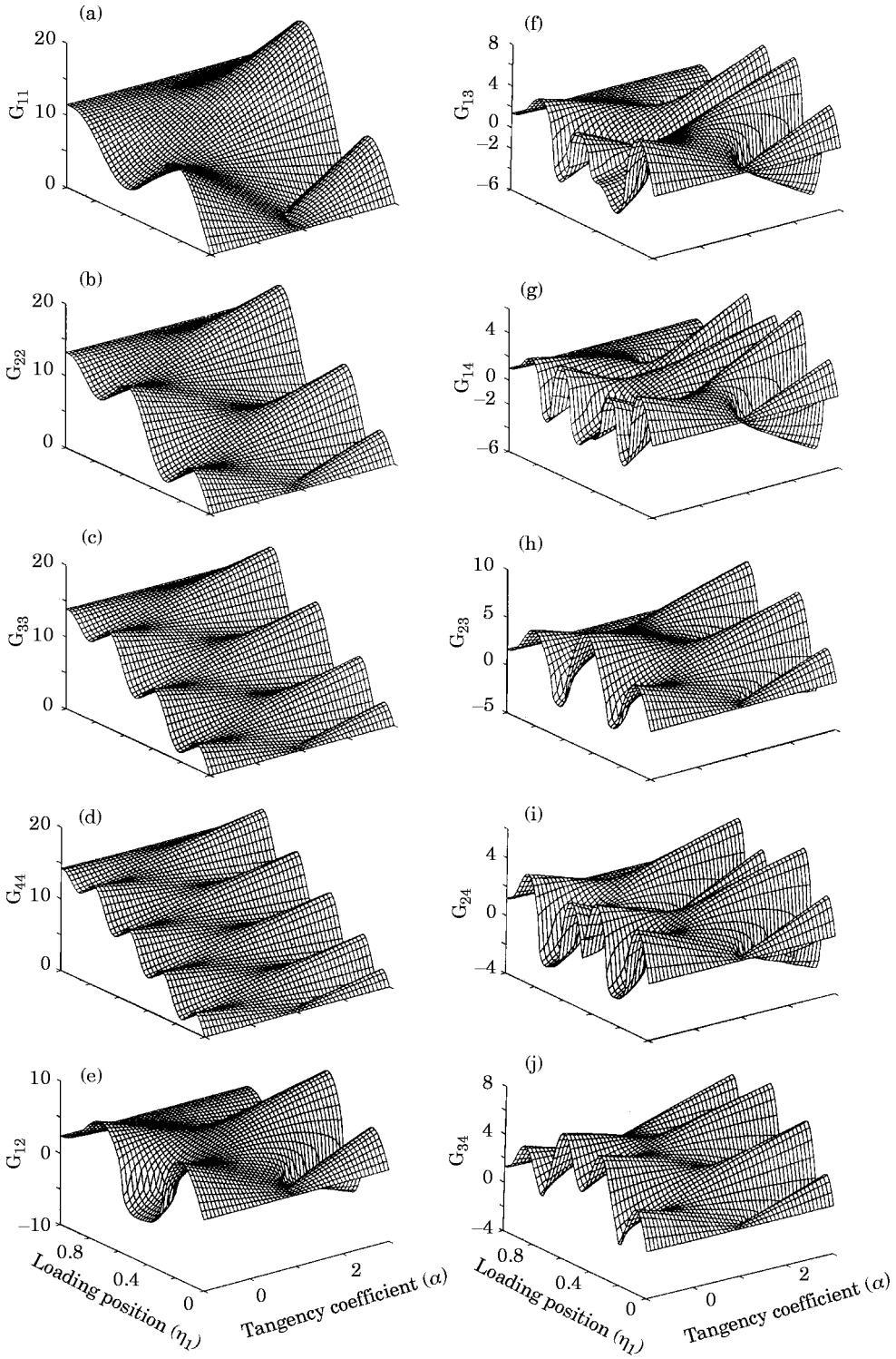

Figure 13. Instability bandwidth parameter, G_{nm}, of a clamped–simply supported column.

4.2. COMBINATION RESONANCE OF THE SUM TYPE

Consider the oscillation of nth and mth modes of equation (8) as

$$\ddot{V}_n(\tau) + \bar{\omega}_n^2 V_n(\tau) = -2\epsilon \cos(\bar{\omega}\tau) f_{nm} V_m(\tau) + RT,$$
$$\ddot{V}_m(\tau) + \bar{\omega}_m^2 V_m(\tau) = -2\epsilon \cos(\bar{\omega}\tau) f_{mn} V_n(\tau) + RT, \tag{17}$$

in which RT represents the regular terms that produce no resonant conditions. Multiplying each equation of equation (17) by $\dot{V}_n$ and $\dot{V}_m$ respectively, and neglecting the regular terms (RT), one obtains the energy form of equation (17)

$$\mathrm{d}/\mathrm{d}t(\tfrac{1}{2}\dot{V}_n^2 + \tfrac{1}{2}\bar{\omega}_n^2 V_n^2) = -2\epsilon \cos(\bar{\omega}\tau) f_{nm} V_m \dot{V}_n,$$
$$\mathrm{d}/\mathrm{d}t(\tfrac{1}{2}\dot{V}_m^2 + \tfrac{1}{2}\bar{\omega}_m^2 V_m^2) = -2\epsilon \cos(\bar{\omega}\tau) f_{mn} V_n \dot{V}_m. \tag{18}$$

The term on the left side of each equation represents the time rate change of the total energy of the nth and mth modes respectively; the term on the right side of each equation represents the power input to the nth and mth modes by the

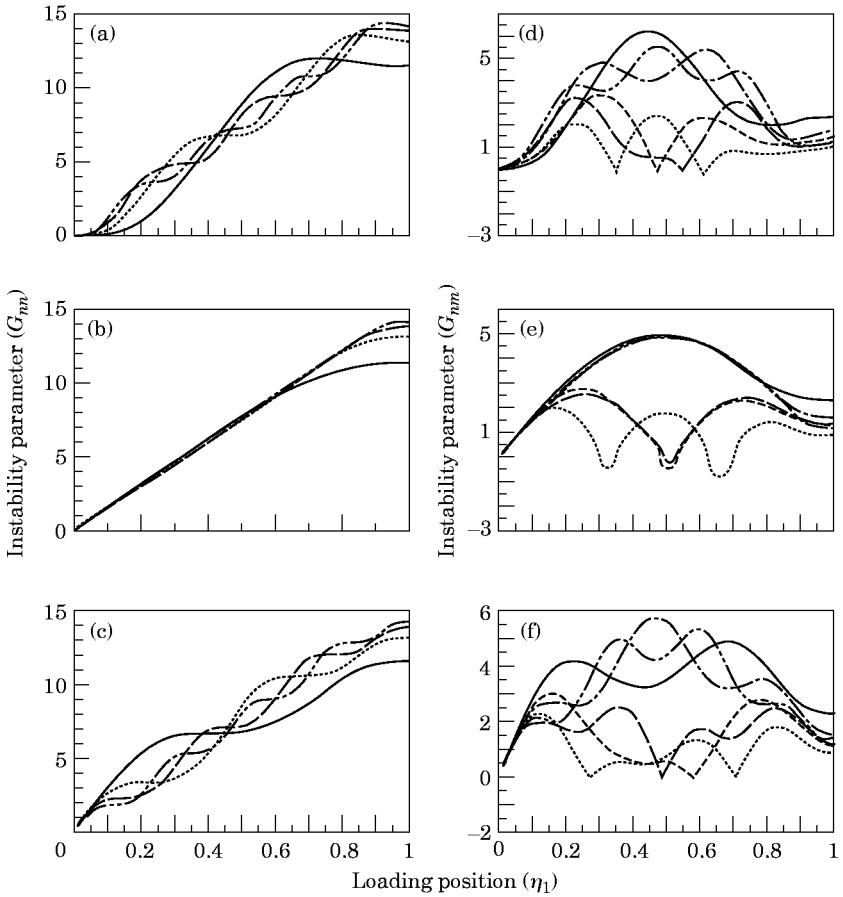

Figure 14. Instability bandwidth parameter, G_{nm}, of a clamped–simply supported column versus loading position η_1. α values and key identical to Figure 5.

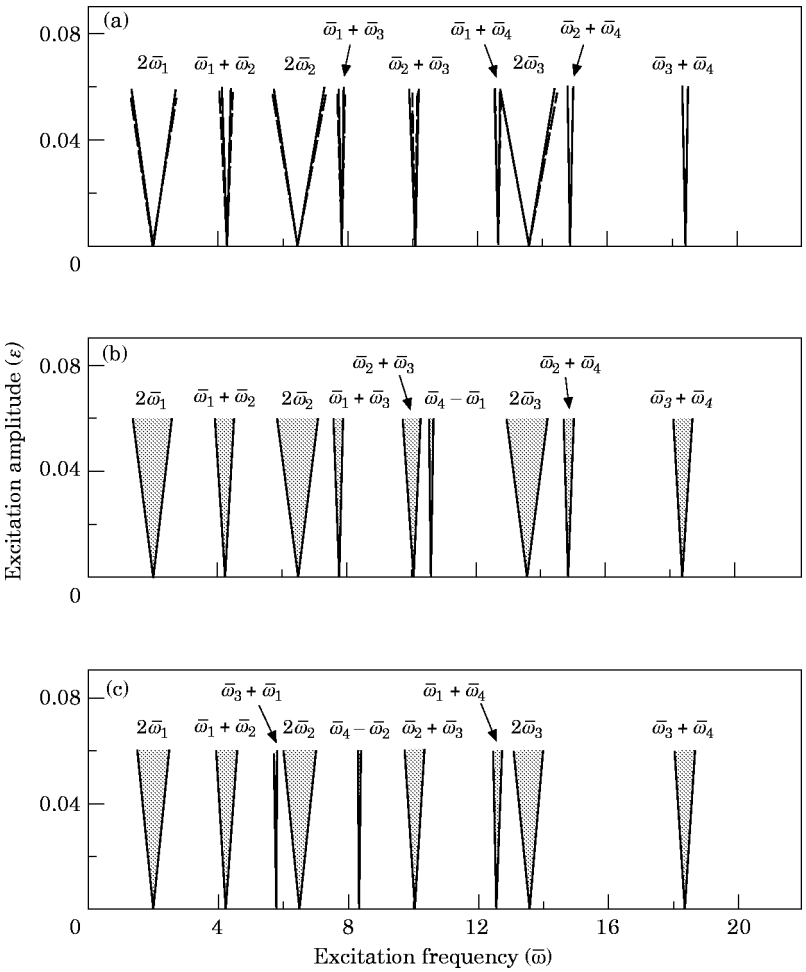

Figure 15. Parametric instability regions of a clamped–simply supported column for various tangency coefficient, α, and loading position, η_1: (a) $\eta_1 = 1{\cdot}0$, α arbitrary; (b) $\eta_1 = 0{\cdot}65$, $\alpha = 0{\cdot}5$; (c) $\eta_1 = 0{\cdot}5$, $\alpha = 0{\cdot}5$. Key as for Figure 11.

generalized forces, $-2\epsilon \cos(\bar{\omega}\tau) f_{nm} V_m$ and $-2\epsilon \cos(\bar{\omega}\tau) f_{mn} V_n$, respectively. As ϵ approaches zero, the power from the generalized forces is small, and thus in a short time interval the oscillation of $V_n(\tau)$ and $V_m(\tau)$ can be expressed approximately as

$$V_n(\tau) \cong \bar{V}_n \cos(\bar{\omega}_n \tau + \theta_n), \qquad V_m(\tau) \cong \bar{V}_m \cos(\bar{\omega}_m \tau + \theta_m) \tag{19}$$

When the excitation frequency $\bar{\omega}$ approaches the summation of the natural frequencies, $\bar{\omega}_n + \bar{\omega}_m$, the power of the generalized forces becomes

$$\begin{aligned}
&-2\epsilon f_{nm} V_m \dot{V}_n \cos(\bar{\omega}\tau) \\
&\cong \epsilon f_{nm} \bar{V}_n \bar{V}_m \bar{\omega}_n \cos[(\bar{\omega}_n + \bar{\omega}_m)\tau] \{\sin[(\bar{\omega}_n + \bar{\omega}_m)\tau + (\theta_n + \theta_m)] \\
&+ \sin[(\bar{\omega}_n - \bar{\omega}_m)\tau + (\theta_n - \theta_m)]\} \\
&= \tfrac{1}{2}\epsilon f_{nm} \bar{V}_n \bar{V}_m \bar{\omega}_n \{\sin[2(\bar{\omega}_n + \bar{\omega}_m)\tau + (\theta_n + \theta_m)] \\
&+ \sin[2\bar{\omega}_n \tau + (\theta_n - \theta_m)] + \sin[2\bar{\omega}_m \tau - (\theta_n - \theta_m)] + \sin(\theta_n + \theta_m)\},
\end{aligned} \tag{20}$$

$$
\begin{aligned}
&-2\epsilon f_{mn} V_n \dot{V}_m \cos(\bar{\omega}\tau) \\
&\quad \cong \epsilon f_{mn} \overline{V}_n \overline{V}_m \bar{\omega}_m \cos[(\bar{\omega}_n + \bar{\omega}_m)\tau]\{\sin[(\bar{\omega}_n + \bar{\omega}_m)\tau + (\theta_n + \theta_m)] \\
&\qquad - \sin[(\bar{\omega}_n - \bar{\omega}_m)\tau + (\theta_n - \theta_m)]\} \\
&\quad = \tfrac{1}{2}\epsilon f_{mn} \overline{V}_n \overline{V}_m \bar{\omega}_m \{\sin[2(\bar{\omega}_n + \bar{\omega}_m)\tau + (\theta_n + \theta_m)] \\
&\qquad + \sin[2\bar{\omega}_n\tau + (\theta_n - \theta_m)] + \sin[2\bar{\omega}_m\tau - (\theta_n - \theta_m)] + \sin(\theta_n + \theta_m)\}. \qquad (21)
\end{aligned}
$$

The average power of the first three terms in the brace of the right side of equations (20) and (21) is equal to zero. When f_{nm} and f_{mn} have the same sign, the power of the last term in the brace of the right side of equations (20) and (21), $\frac{1}{2}\epsilon f_{nm}\overline{V}_n\overline{V}_m\bar{\omega}_n \sin(\theta_n + \theta_m)$ and $\frac{1}{2}\epsilon f_{mn}\overline{V}_n\overline{V}_m\bar{\omega}_m \sin(\theta_n + \theta_m)$, must have the same sign, too. When they are positive, the power input to the nth and mth modes is positive and the total energy of the nth and mth modes increases continuously. Therefore, the system becomes unstable when the excitation frequency $\bar{\omega}$ is near $\bar{\omega}_n + \omega_m$; however, when f_{nm} and f_{mn} have the opposite signs, this conclusion does not hold.

4.3. COMBINATION RESONANCE OF THE DIFFERENCE TYPE

A similar procedure as above indicates that when f_{nm} and f_{mn} have opposite signs and the excitation frequency $\bar{\omega}$ is near $\bar{\omega}_n - \bar{\omega}_m$, $\bar{\omega}_n > \bar{\omega}_m$, the system becomes unstable.

5. RESULTS AND DISCUSSION

The columns with four different supporting conditions are investigated by applying the general formula developed in the previous section to demonstrate the instability regions of simple and combination resonances. For simplicity, the columns were chosen to have uniform cross-section with length L, mass M, mass per unit length ρ, bending rigidity EI, and fixed supporting point O. The columns were subjected to a sinusoidal periodic load $f(t) = f_0 \cos \omega t$ at an arbitrary loading point P in the direction of the tangency coefficient α. The natural frequencies $\bar{\omega}_n$ and corresponding normalized mode shape functions $\phi_n(\eta)$ of each column are obtained first from equation (1) with corresponding boundary conditions.

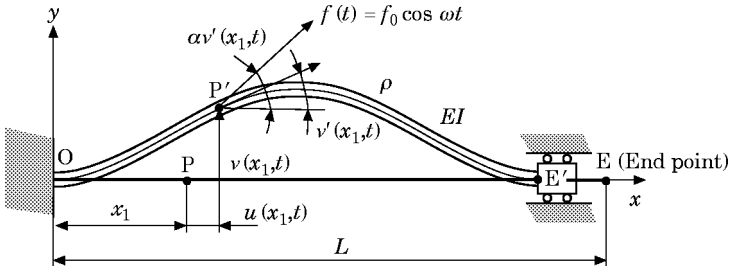

Figure 16. Parametric excitation of a clamped–clamped column. $\lambda_1 = 4{\cdot}73004$; $\lambda_2 = 7{\cdot}85321$; $\lambda_3 = 10{\cdot}99561$; $\lambda_4 = 14{\cdot}13717$; $\bar{\omega}_n = \lambda_n^2/\lambda_1^2$; $\phi_n = \sqrt{1/\rho L}\{\cosh(\lambda_n\eta) - \cos(\lambda_n\eta) - k_n[\sinh(\lambda_n\eta) - \sin(\lambda_n\eta)]\}$, where $k_n = [\cosh(\lambda_n) - \cos(\lambda_n)]/[\sinh(\lambda_n) - \sin(\lambda_n)]$.

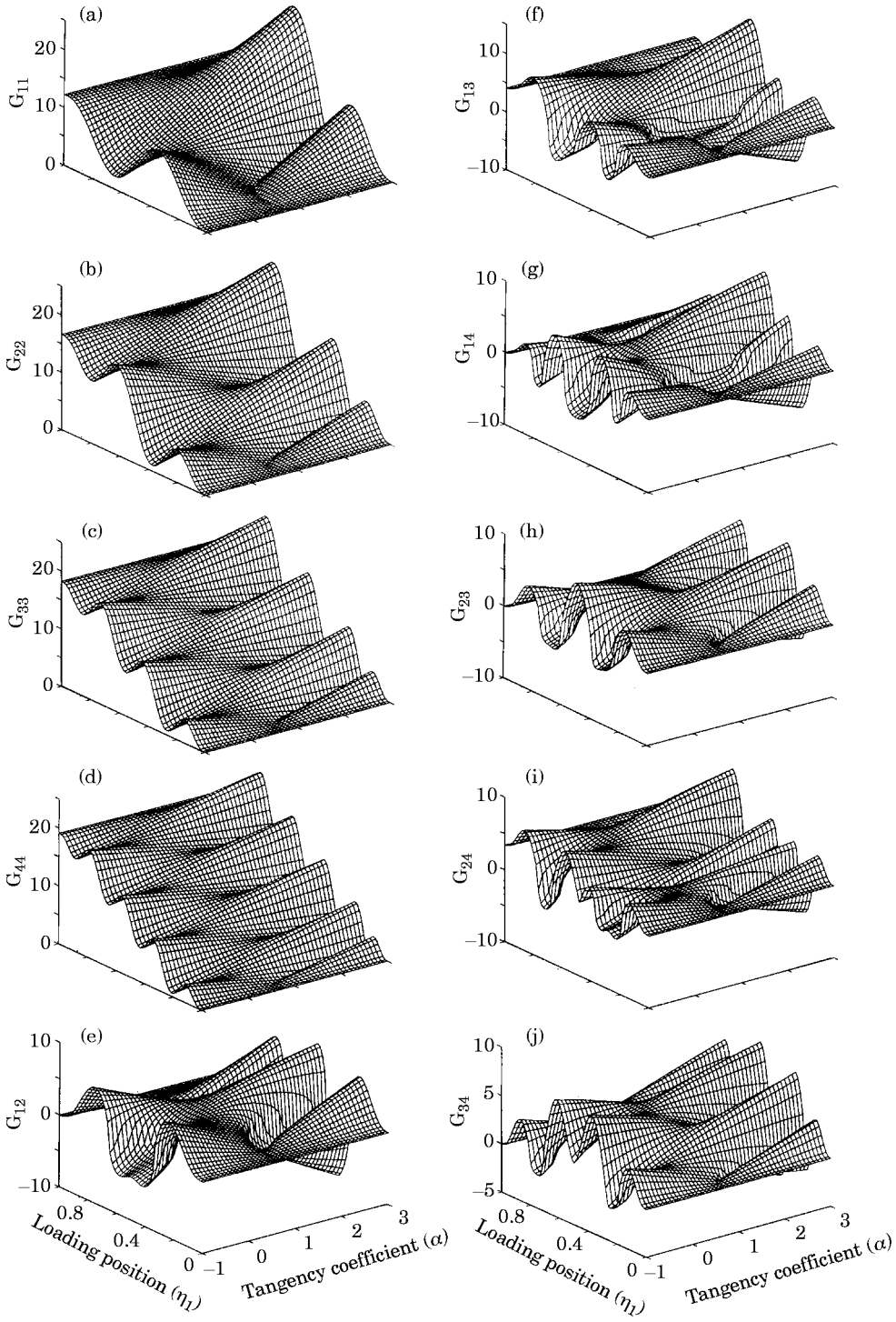

Figure 17. Instability bandwidth parameter, G_{nm}, of a clamped–clamped column.

Substituting $\bar{\omega}_n$ and corresponding $\phi_n(\eta)$ into equations (9) and (10), the instability bandwidth parameters G_{nm} with varying values of the tangency coefficient α at the non-dimensionalized loading position η_1 were found. The results of the instability bandwidth parameters G_{nm} are presented. Several G_{nm} curves with varying values of α or η_1 and several instability diagrams with specified α and η_1 are plotted. The instability bandwidth parameters G_{nm}, n, $m = 1, 2, 3$, and 4, are presented without loss of generality.

5.1. CASE I: CANTILEVERED COLUMN

A cantilevered column under periodic load is shown in Figure 2, in which the non-dimensionlized natural frequencies $\bar{\omega}_n$ and normalized mode shape functions $\phi_n(\eta)$ are also shown. The instability bandwidth parameters G_{nm}, $n, m = 1, 2, 3$, and 4, varying with the tangency coefficient α and the loading position η_1, are partly shown in Figures 3(a–j), respectively. As one can see, each G_{nm} surface has many wrinkles, and the values of G_{nm} vary rapidly with respect to α and η_1 in all α–η_1 planes. In Figures 4(a–d) the sectional views of G_{nn} and G_{nm} curves are shown for the loading position $\eta_1 = 1{\cdot}0$ and $0{\cdot}8$ respectively. In Figures 5(a–f) the sectional views of G_{nn} and G_{nm} curves are shown for the tangency coefficient $\alpha = 1{\cdot}0$, $0{\cdot}5$, and $0{\cdot}0$ respectively. In Figures 4 and 5, all the G_{nm} curves are different as the loading point or the tangency coefficient are varied. The present results shown in Figure 4(a, c) are the same as those obtained by Chen and Yeh [14] for a cantilevered column under periodic loads in the direction of the tangency coefficient for $\eta_1 = 1{\cdot}0$. In Figures 5(c, f) the direction of the periodic load is parallel to the undeformed horizontal axis (the tangency coefficient $\alpha = 0$). The value of each G_{nn} for simple resonance increases as the distance between the fixed

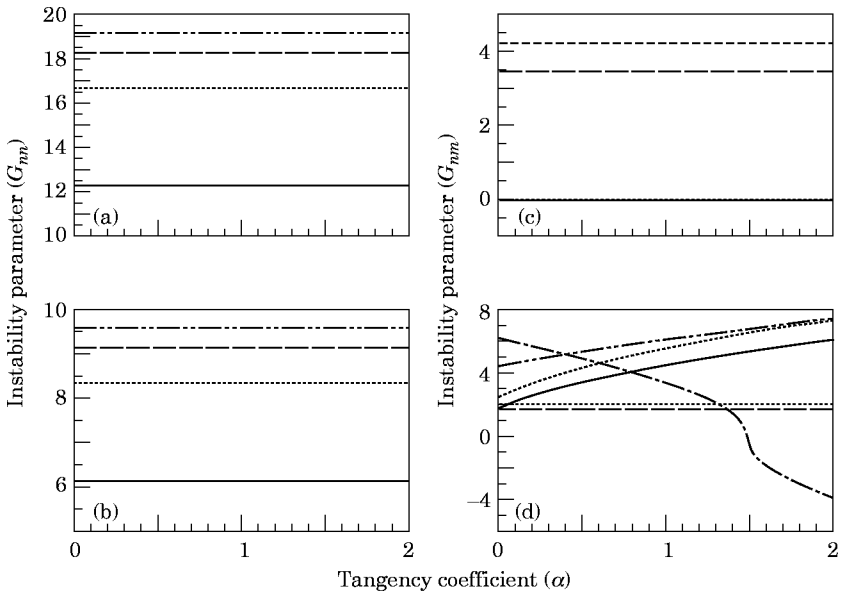

Figure 18. Instability bandwidth parameter, G_{nm}, of a clamped–clamped column versus tangency coefficient, α. (a) $\eta_1 = 1{\cdot}0$, key as for Figure 4(a); (b) $\eta_1 = 0{\cdot}5$, key as for Figure 4(a); (c) $\eta_1 = 1{\cdot}0$, key as for Figure 4(c); (d) $\eta_1 = 0{\cdot}5$, key as for Figure 4(c).

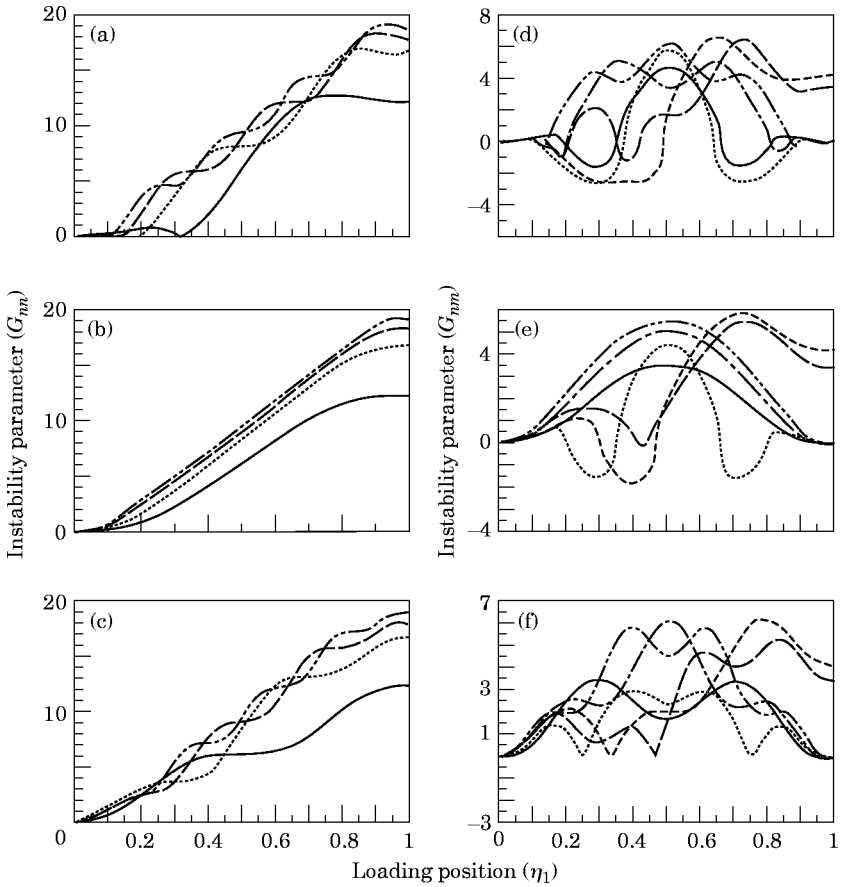

Figure 19. Instability bandwidth parameter, G_{nm}, of clamped–clamped column versus loading position, η_1. (a, d), $\alpha = 1{\cdot}0$; (b, e), $\alpha = 0{\cdot}5$; (c, f), $\alpha = 0{\cdot}0$. Key: (a, b, c) as for Figure 4(a); (d, e, f) as for Figure 4(c).

supporting point and the loading point increases; the instability parameters G_{nm} for combination resonance are always greater than or equal to zero. For specific tangency coefficient α and loading position η_1, the instability diagram can be plotted by using the values of instability bandwidth parameters G_{nm}, the natural frequencies $\bar{\omega}_n$, $\bar{\omega}_m$ and the amplitude of excitation ϵ. Figures 6(a–c) show the instability diagram for $\eta_1 = 1$ and $\alpha = \phi$, $\eta_1 = 1$ and $\alpha = 0$, as well as $\eta_1 = 0{\cdot}7$ and $\alpha = 0$, respectively. The instability regions are quite different with varying η_1 or α. Figure 6(a) shows that the present results have no discernible difference from those of Iwatsubo *et al*. [12] and Nayfeh and Mook [2] on the same ordinate scale.

5.2. CASE II: SIMPLY SUPPORTED COLUMN

A simply supported column under periodic load is shown in Figure 7. The instability bandwidth parameters G_{nm} $n, m = 1, 2, 3,$ and 4 varying with the

tangency coefficient α and the loading position η_1 are partly shown in Figures 8(a–j), respectively. It is noted that

(1) All the odd mode shape functions, $\phi_n(\eta) = \sqrt{2/\rho L}\sin n\pi\eta$ are symmetric about the center point $\eta = 0{\cdot}5$, and the even mode shape functions skewsymmetric about $\eta = 0{\cdot}5$. Moreover, all the derivatives of the mode shape functions $\phi_n'(\eta)$ are orthogonal in the interval of [0, 1]. Recalling equation (9), when the tangency coefficient α is constant and $n \neq m$, the parametric excitation coefficient $f_{nm}(\eta_1)$ becomes

$$f_{nm}(\eta_1) = M\left[\int_0^{\eta_1} \phi_n'(\eta)\phi_m'(\eta)\,\mathrm{d}\eta - \alpha\phi_n(\eta_1)\phi_m'(\eta_1)\right]$$

$$= M\left[-\int_{\eta_1}^{1} \phi_n'(\eta)\phi_m'(\eta)\,\mathrm{d}\eta - \alpha\phi_n(\eta_1)\phi_m'(\eta_1)\right]$$

$$= \left\{\begin{array}{l} -M\left[\displaystyle\int_0^{1-\eta_1} \phi_n'(\eta)\phi_m'(\eta)\,\mathrm{d}\eta - \alpha\phi_n(1-\eta_1)\phi_m'(1-\eta_1)\right],\ (n+m)\ \text{even},\\ +M\left[\displaystyle\int_0^{1-\eta_1} \phi_n'(\eta)\phi_m'(\eta)\,\mathrm{d}\eta - \alpha\phi_n(1-\eta_1)\phi_m'(1-\eta_1)\right],\ (n+m)\ \text{odd}, \end{array}\right\}$$

$$= \left\{\begin{array}{ll} -f_{nm}(1-\eta_1), & (n+m)\ \text{even},\\ +f_{nm}(1-\eta_1), & (n+m)\ \text{odd}. \end{array}\right\} \tag{22}$$

Therefore, the parametric excitation coefficient $f_{nm}(\eta_1)$, $n \neq m$, is symmetric for odd $n + m$ and skewsymmetric for even $n + m$ about $\eta_1 = 0{\cdot}5$. From equation (10), all of the combination resonance instability parameters G_{nm} are symmetric to the plane of $\eta_1 = 0{\cdot}5$, as shown in Figures 8(e–j).

(2) When the loading point is located at the right end of the column, $\eta_1 = 1$, this point is constrained by the supported condition so that all of the mode shape functions $\phi_n(\eta)$ vanish at $\eta_1 = 1$. Moreover, all of the derivatives of the mode shape functions $\phi_n'(\eta)$ are orthogonal in the interval of [0, 1], then

$$f_{nm} = M\left[\int_0^{1} \phi_n'(\eta)\phi_m'(\eta)\,\mathrm{d}\eta - \alpha\phi_n(1)\phi_m'(1)\right]$$

$$= M\left[\int_0^{1} \phi_n'(\eta)\phi_m'(\eta)\,\mathrm{d}\eta\right] = n^2\pi^2\delta_{nm}. \tag{23}$$

Therefore, all of the combination resonance instability parameters G_{nm}, $n \neq m$ vanish and all of the simple resonance instability parameters G_{nn} have the same value of π^2.

(3) When the position of loading point is located at the midpoint of the column, $\eta_1 = 0{\cdot}5$, the values of mode shape functions $\phi_n(\eta_1)$ are zero for $n = 2, 4, 6, \ldots$ and the derivatives of mode shape functions $\phi_n'(\eta_1)$ are zero for $n = 1, 3, 5, \ldots$. The parametric excitation coefficient $f_{nn}(\eta_1)$ becomes

$$f_{nn} = M\left[\int_0^{0{\cdot}5} \phi_n'^2(\eta)\,\mathrm{d}\eta - \alpha\phi_n(0{\cdot}5)\phi_n'(0{\cdot}5)\right] = M\left[\int_0^{0{\cdot}5} \phi_n'^2(\eta)\,\mathrm{d}\eta\right] = 0{\cdot}5n^2\pi^2, \tag{24}$$

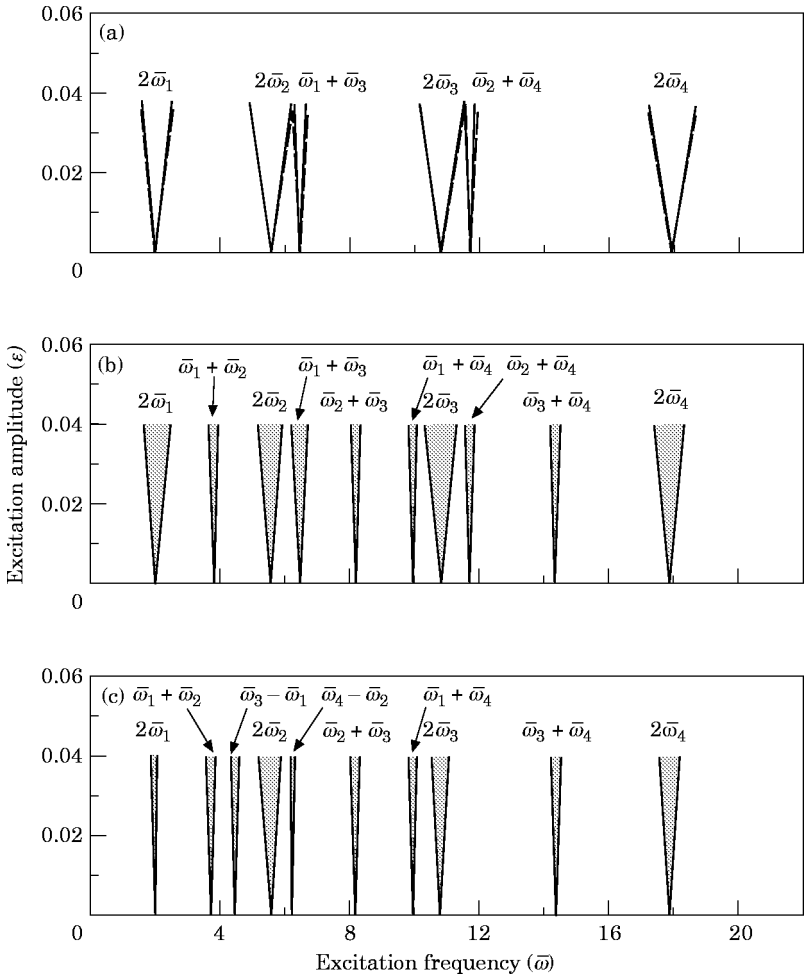

Figure 20. Parametric instability regions of a clamped–clamped column for various tangency coefficients, α, and loading position. η_1. (a) $\eta_1 = 1{\cdot}0$, α arbitrary; (b) $\eta_1 = 0{\cdot}6$, $\alpha = 1{\cdot}0$; (c) $\eta_1 = 0{\cdot}4$, $\alpha = 1{\cdot}0$. Key as for Figure 11.

and when $n \neq m$ and $(n + m)$ even, $f_{nm}(\eta)$ becomes

$$f_{nm} = M\left[\int_0^{0\cdot5} \phi_n'(\eta)\phi_m'(\eta)\,\mathrm{d}\eta - \alpha\phi_n(0\cdot5)\phi_m'(0\cdot5)\right] = M\left[\int_0^{0\cdot5} \phi_n'(\eta)\phi_m'(\eta)\,\mathrm{d}\eta\right]$$

$$= 2n^2\pi^2\left[\int_0^{0\cdot5} \cos(n\pi\eta)\cos(m\pi\eta)\,\mathrm{d}\eta\right] = 0. \tag{25}$$

Thus, all of the simple resonance instability parameters G_{nn} have the same value $0\cdot5\pi^2$ and the combination resonance instability parameters G_{nm} vanish when $\eta_1 = 0\cdot5$ and $(n + m)$ even.

(4) When the tangency coefficient $\alpha = 0\cdot5$ and the loading point is located at η_1 the parametric excitation coefficients f_{nn} become

$$f_{nn} = M\left[\int_0^{\eta_1} \phi_n'^2(\eta)\,\mathrm{d}\eta - 0\cdot5\phi_n(\eta_1)\phi_n'(\eta_1)\right] = n^2\pi^2\eta_1. \tag{26}$$

From equation (10), all the simple resonance instability parameters G_{nn} overlap and became a straight line segment with the same value $\pi^2\eta_1$.

Figures 9(a, b) show G_{nm} curves varying with the tangency coefficient α for the loading position $\eta_1 = 0\cdot5$; all of the simple resonance instability parameters G_{nn} have the same value $0\cdot5\pi^2$ and the combination resonance instability parameters G_{13} and G_{24} vanish. Figures 10(a–f) show that G_{nm} values vary with the loading position η_1 for the tangency coefficient $\alpha = 1\cdot0$, $0\cdot5$, and $0\cdot0$, respectively. In Figure 10 all of the combination resonance instability parameters G_{nm} are symmetric about $\eta_1 = 0\cdot5$. When the loading position is located at the right end of the column, $\eta_1 = 1$, all the simple resonance instability parameters G_{nn} have the same value π^2 for all values of the tangency coefficient and all the combination resonances instability parameters G_{nm} vanish. When $\alpha = 0\cdot5$, all of the simple resonance instability parameters G_{nn} overlap and form a straight line of $\pi^2\eta_1$ as shown in Figure 10(b). Figures 11(a–c) show the instability diagram for $\eta_1 = 1$ with arbitrary α, $\eta_1 = 0\cdot67$ with $\alpha = 0\cdot5$, and $\eta_1 = 0\cdot5$ with $\alpha = 0\cdot5$, respectively. Figure 11(a) shows that all of the combination resonances vanish and the present results have no discernible difference from the results obtained by Iwatsubo *et al*. [12] on the same ordinate scale. When the loading point is not located at the end of the column, the combination resonances may occur as shown in Figures 11(b) and 11(c).

5.3. CASE III: CLAMPED SIMPLY-SUPPORTED COLUMN

A clamped–simply supported column under periodic load is shown in Figure 12. The instability bandwidth parameters G_{nm}, $n, m = 1, 2, 3$, and 4, varying with the tangency coefficient α and the loading position η_1 are shown in Figures 13(a–j) respectively. The G_{nm} surfaces vary more rapidly with respect to α and η_1 in all plots.

In Figures 14(a–f), the G_{nm} curves are shown to vary with the loading position for the tangency coefficient $\alpha = 1{\cdot}0$, $0{\cdot}5$, and $0{\cdot}0$ respectively. When $\alpha = 1{\cdot}0$, all the combination resonance instability parameters G_{nm} are almost greater than or equal to zero as shown in Figures 14(d). When $\alpha = 0{\cdot}5$, all of the simple resonance instability parameters G_{nn} almost overlap and form a straight line in the range of $0 \leqslant \eta_1 \leqslant 0{\cdot}6$ as shown in Figure 14(b). Figures 15(a–c) show the instability diagram for $\eta_1 = 1$ with arbitrary α, $\eta_1 = 0{\cdot}65$ with $\alpha = 0{\cdot}5$, and $\eta_1 = 0{\cdot}5$ with $\alpha = 0{\cdot}5$, respectively. The present results, in Figure 15(a) can be seen to be close to those of Iwatsubo *et al*. [12] for the end loading case. The instability bandwidth regions become different when changing the loading condition η_1 or the tangency coefficient α.

5.4. CASE IV: CLAMPED–CLAMPED COLUMN

Figure 16 shows a clamped–clamped column under periodic load. The instability bandwidth parameters G_{nm}, $n, m = 1, 2, 3$, and 4, varying with the tangency coefficient α and the loading position η_1 are shown in Figures 17(a–j), respectively. It is noted that

(1) All the odd mode shape functions $\phi_n(\eta)$ are symmetric about $\eta = 0{\cdot}5$ and all the even mode shape functions skewsymmetric about $\eta = 0{\cdot}5$. The derivatives of the mode shape functions $\phi_n'(\eta)$, $\phi_m'(\eta)$ are orthogonal to each other in the interval of [0, 1] for $(n + m)$ odd. From equation (9) , when $n \neq m$, $(n + m)$ odd and constant α, the parametric excitation coefficients $f_{nm}(\eta_1)$ become

$$f_{nm}(\eta_1) = M\left[\int_0^{\eta_1} \phi_n'(\eta)\phi_m'(\eta)\,\mathrm{d}\eta - \alpha\phi_n(\eta_1)\phi_m'(\eta_1)\right]$$

$$= M\left[-\int_{\eta_1}^{1} \phi_n'(\eta)\phi_m'(\eta)\,\mathrm{d}\eta - \alpha\phi_n(\eta_1)\phi_m'(\eta_1)\right]$$

$$= M\left[\int_0^{1-\eta_1} \phi_n'(\eta)\phi_m'(\eta)\,\mathrm{d}\eta - \alpha\phi_n(1-\eta_1)\phi_m'(1-\eta_1)\right]$$

$$= f_{nm}(1 - \eta_1). \tag{27}$$

that is, the parametric excitation coefficients $f_{nm}(\eta_1)$ are symmetric about $\eta_1 = 0{\cdot}5$. From equation (10), the combination resonance instability parameters G_{nm} are symmetric to the plane of $\eta_1 = 0{\cdot}5$ for odd $(n + m)$, as shown in Figures 17(e), 17(g), 17(h), and 17(j).

(2) When the loading point is located at the right clamped end of the column, $\eta_1 = 1$, all the mode shape functions $\phi_n(\eta)$ and its derivatives $\phi_n'(\eta)$ vanish. Moreover, the derivatives of the mode shape functions $\phi_n'(\eta)$, $\phi_m'(\eta)$ are orthogonal to each other in the interval of [0, 1] for $n \neq m$ and odd $(n + m)$, i.e.,

$$f_{nm} = M\left[\int_0^1 \phi_n'(\eta)\phi_m'(\eta)\,\mathrm{d}\eta - \alpha\phi_n(1)\phi_m'(1)\right] = M\left[\int_0^1 \phi_n'(\eta)\phi_m'(\eta)\,\mathrm{d}\eta\right] = 0. \tag{28}$$

Therefore, when $\eta = 1$, the combination resonance instability parameters G_{nm} vanish for odd $(n + m)$.

(3) When the loading point is located at the midpoint of the column, i.e., $\eta_1 = 0{\cdot}5$. The mode shape functions $\phi_n(\eta_1)$ are zero for $n = 2, 4, 6, \ldots$ and the derivatives of the mode shape functions $\phi_n'(\eta_1)$ are zero for $n = 1, 3, 5, \ldots$. The parametric excitation coefficient $f_{nn}(\eta)$ becomes

$$f_{nn} = M\left[\int_0^{0{\cdot}5} \phi_n'^2(\eta)\,\mathrm{d}\eta - \alpha\phi_n(0{\cdot}5)\phi_n'(0{\cdot}5)\right] = M\left[\int_0^{0{\cdot}5} \phi_n'^2(\eta)\,\mathrm{d}\eta\right]. \tag{29}$$

Furthermore, when $n \neq m$ and even $(n + m)$, $f_{nm}(\eta)$ becomes

$$f_{nm} = M\left[\int_0^{0{\cdot}5} \phi_n'(\eta)\phi_m'(\eta)\,\mathrm{d}\eta - \alpha\phi_n(0{\cdot}5)\phi_m'(0{\cdot}5)\right] = M\left[\int_0^{0{\cdot}5} \phi_n'(\eta)\phi_m'(\eta)\,\mathrm{d}\eta\right]. \tag{30}$$

Thus, all of the simple resonance instability parameters G_{nn} and the combination resonance instability parameters G_{nm} with even $(n + m)$ are independent of the tangency coefficient.

In Figures 18(a–d), the G_{nm} curves varying with the tangency coefficient are shown for the loading position $\eta_1 = 1{\cdot}0$ and $\eta_1 = 0{\cdot}5$ respectively. In Figures 18(a, c), all the simple and combination resonance instability parameters G_{nm} are independent of the tangency coefficient; the combination resonance instability parameters G_{12}, G_{14}, G_{23} and G_{34} vanish. In Figure 18(b, d), all the simple resonance instability parameters G_{nn} and the combination resonance instability parameters G_{13} and G_{24} are independent of the tangency coefficient. Figure 19 shows the G_{nm} curves for the tangency coefficient $\alpha = 1{\cdot}0$, $0{\cdot}5$, and $0{\cdot}0$ respectively. The combination resonance instability parameters G_{12}, G_{14}, G_{23} and G_{34} are symmetric about $\eta_1 = 0{\cdot}5$. Figure 20 shows the instability diagrams for $\eta_1 = 1$ with arbitrary α, $\eta_1 = 0{\cdot}6$ with $\alpha = 1{\cdot}0$, and $\eta_1 = 0{\cdot}4$ with $\alpha = 1{\cdot}0$, respectively. In Figure 20(a) the conbination resonances G_{12}, G_{14}, G_{23} and G_{34} vanish and the present instability bandwidths can be seen to have no discernible difference from those of Iwatsubo *et al*. [12] for the end loading case. When the loading point is not located at the end of the column, the combination resonances may occur as shown in Figures 20(b, c).

6. CONCLUSIONS

The parametrically excited instability behavior of a general column has been investigated analytically. The column may have non-uniform cross-section, non-homogeneous material, or various supported conditions, and is subjected to a periodic load in varying direction of the tangency coefficient at an arbitrary axial position on the column. The instability bandwidths of simple and combination resonances can be determined by a general formula derived in this paper. In the formula, the instability bandwidth parameters G_{nm} are functions of the natural frequencies, the normalized natural mode shapes of the column, the length and

mass of the column, the fixed supporting position, the loading position, and the tangency coefficient. Physical explanations have been given for the behavior of parametric resonances and the following conclusions can be drawn.

(1) When the tangency coefficient $\alpha = 0$, for any fixed supporting position and loading position, all of the combination resonances, if occurring, are of the sum type.

(2) With $\alpha = 0$ and constant excitation amplitude parameter ϵ, the bandwidth of simple resonance increases with increasing distance between the fixed supporting point and loading point.

(3) When the loading point is at a constrained point where the transverse deflection or the tangent slope of the column at this point is zero, the instability behavior of the column is independent of the tangency coefficient, and all the combination resonances, if occurring, are of the sum type.

REFERENCES

1. C. S. Hsu 1963 *Journal of Applied Mechanics* **30**, 367–372. On the parametric excitation of a dynamic system having multiple degrees of freedom.
2. A. H. Nayfeh and D. T. Mook 1977 *Journal of Acoustical Society of America* **62**, 375–381. Parametric excitations of linear systems having many degrees of freedom.
3. T. Yamamoto and A. Saito 1967 *Transactions of the Japan Society of Mechanical Engineers* **33**, 905–914. On the oscillations of summed and differential types under parametric excitation.
4. K. L. Handoo and V. Sundararajan 1971 *Journal of Sound and Vibration* **18**, 45–53. Parametric instability of a cantilevered column with end mass.
5. H. Saito and N. Koizumi 1982 *International Journal of Mechanical Sciences* **24**, 755–761. Parametric vibrations of a horizontal beam with a concentrated mass at one end.
6. K. W. Buffinton and T. R. Kane 1985 *International Journal of Solids and Structures* **21**, 617–643. Dynamics of a beam moving over supports.
7. R. Elmaraghy and B. Tabarrok 1975 *Journal of the Franklin Institute* **300**, 25–39. On the dynamic stability of an axially oscillating beam.
8. H. A. Evensen and R. M. Evan-Iwanowski 1966 *Journal of Applied Mechanics* **33**, 141–148. Effects of longitudinal inertia upon the parametric response of elastic columns.
9. V. V. Bolotin 1964 *The Dynamic Stability of Elastic Systems*. San Francisco: Holden-Day.
10. T. Iwatsubo, Y. Sugiyama and K. Ishihara 1972 *Journal of Sound and Vibration* **23**, 245–257. Stability and non-stationary vibration of columns under periodic loads.
11. T. Iwatsubo, M. Saigo and Y. Sugiyama 1973 *Journal of Sound and Vibration* **30**, 65–77. Parametric instability of clamped–clamped and clamped–simply supported columns under periodic axial load.
12. T. Iwatsubo, Y. Sugiyama and Ogino 1974 *Journal of Sound and Vibration* **33**, 211–221. Simple and combination resonances of columns under periodic axial loads.
13. K. Sato, H. Saito and K. Otomi 1978 *Journal of Applied Mechanics* **45**, 643–648. The parametric response of a horizontal beam carrying a concentrated mass under gravity.
14. C. C. Chen and M. K. Yeh 1995 *Journal of Sound and Vibration* **183**, 253–267. Parametric instability of a cantilevered column under periodic loads in the direction of the tangency coefficient.